Supplementary Information

Spider hanging inside a carbon cage: off-center shift and pyramidalization of Sc_3N clusters inside C_{84} and C_{86} fullerene cages

Ze Fu,‡ Min Guo,‡ Yang-Rong Yao,‡ Qingyu Meng, Yingjing Yan, Qin Wang, Yi Shen and Ning Chen*

*College of Chemistry, Chemical Engineering and Materials Science, and State Key Laboratory of Radiation Medicine and Protection, Soochow University, Suzhou, Jiangsu 215123, P. R. China

‡These authors contribute equally to this work.

Table of Contents

High-performance liquid chromatography (HPLC) isolation of $Sc_3N@C_{2n}$ (2n = 84, 86)

$Sc_3N@C_{2n}$ (2n = 84, 86) were purified by HPLC processes with UV detection at 310 nm using toluene as the mobile phase.

$Sc_3N@C_s(51365)\text{-}C_{84}$ was purified by a four-stage HPLC process, as shown in Figure S1. The first stage was performed on a Buckyprep-M column (25 mm × 250 mm, Cosmosil Nacalai Tesque) with a 13 mL / min flow rate. After that, the fraction from 32.1 to 60 min was re-injected into a Buckyprep column (10 mm × 250 mm, Cosmosil Nacalai Tesque) for the second stage separation with a 4 mL / min flow rate. The fraction from 139.3 to 179.9 min, which contained $Sc_3N@C_s(51365)\text{-}C_{84}$ was collected. The third stage of separation was conducted on a 5PBB column (10 mm × 250 mm, Cosmosil Nacalai Tesque) with a 4 mL / min flow rate. The fraction from 157.8 to 184.5 min, which contained $Sc_3N@C_s(51365)\text{-}C_{84}$ was collected. The final stage was performed on a Buckyprep-M column (10 mm × 250 mm, Cosmosil Nacalai Tesque) with a 4 mL/min flow rate to purify $Sc_3N@C_s(51365)\text{-}C_{84}$. After four rounds of isolation, the fraction from 53.8 to 64.1 min containing pure $Sc_3N@C_s(51365)\text{-}C_{84}$ was collected and stored for characterizations.

$Sc_3N@D_3(19)\text{-}C_{86}$ was purified by a six-stage HPLC process, as shown in Figure S2. The first stage was performed on a Buckyprep-M column (25 mm × 250 mm, Cosmosil Nacalai Tesque) with a 13 mL / min flow rate. After that, the fraction from 35.9 to 60 min was re-injected into a Buckyprep column (10 mm × 250 mm, Cosmosil Nacalai Tesque) for the second stage separation with a 4 mL / min flow rate. The fraction from 110.1 to 123.7 min, which contained $Sc_3N@D_3(19)\text{-}C_{86}$ was collected. The third stage of separation was conducted on a 5PBB column (10 mm × 250 mm, Cosmosil Nacalai Tesque) with a 4 mL / min flow rate. The fraction from 134.2 to 154.6 min, which contained $Sc_3N@D_3(19)\text{-}C_{86}$ was collected. The fourth stage of separation was conducted on a Buckyprep-M column (10 mm × 250 mm, Cosmosil Nacalai Tesque) with a 4 mL / min flow rate. The fraction from 41.3 to 53.3 min, which contained $Sc_3N@D_3(19)\text{-}C_{86}$ was collected. The fifth stage of separation was conducted on a Buckyprep-D column (10 mm × 250 mm, Cosmosil Nacalai Tesque) with a 4 mL / min flow rate. The fraction from 32.4 to 41.8 min, which contained $Sc_3N@D_3(19)\text{-}C_{86}$ was collected. The final stage was performed on a Buckyprep-M column (10 mm × 250 mm, Cosmosil Nacalai Tesque) with a 4 mL/min flow rate under the recycle mode to purify $Sc_3N@D_3(19)\text{-}C_{86}$. After six rounds of isolation, the fraction from 107.5 to 118.1 min containing pure $Sc_3N@D_3(19)\text{-}C_{86}$ was collected and stored for characterizations.

In total 1.97 g of graphite powder and 1.02 g of Sc_2O_3 (molar ratio of C:Sc = 15:1) were packed in each rod. On average ca. 20 mg of crude fullerene mixture per rod was obtained and totally 200 carbon rods were vaporized in this work. The crude fullerene mixtures include empty fullerenes such as C_{60}, C_{70}, C_{82}, C_{90}, C_{100}, and C_{120}, and endohedral metallofullerenes such as $Sc_3N@C_{2n}$ (2n = 68, 78, 80, 82, 84, 86) and $Sc_2C_2@C_{2n}$ (2n = 68, 72, 74, 80, 82, 84, 86, 88). After HPLC isolation and purification process, ca. 0.13 mg purified $Sc_3N@C_s(51365)\text{-}C_{84}$ and ca. 0.06 mg purified $Sc_3N@D_3(19)\text{-}C_{86}$ were obtained.

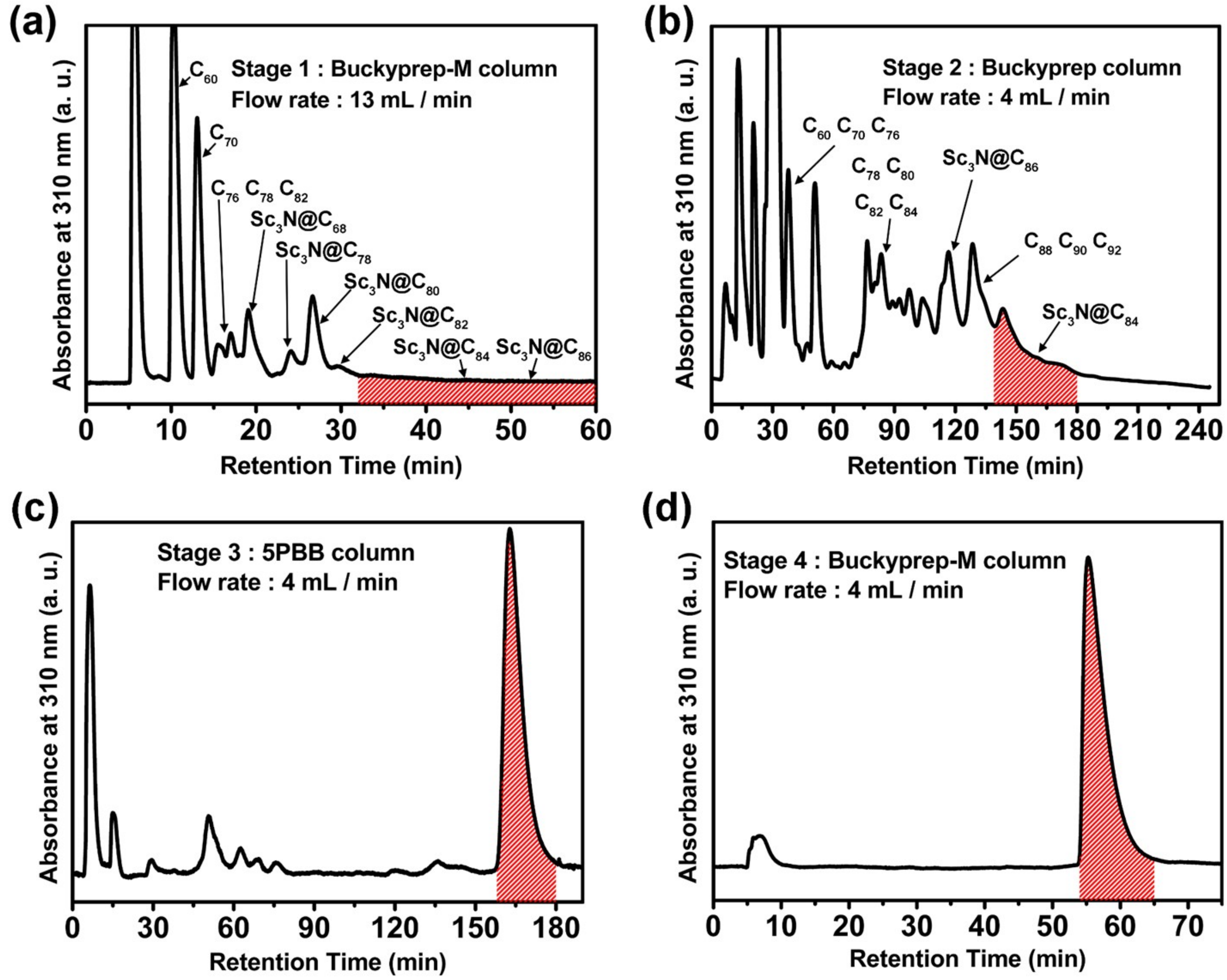

Fig. S1 HPLC isolation procedures of $Sc_3N@C_s(51365)$-C_{84}.

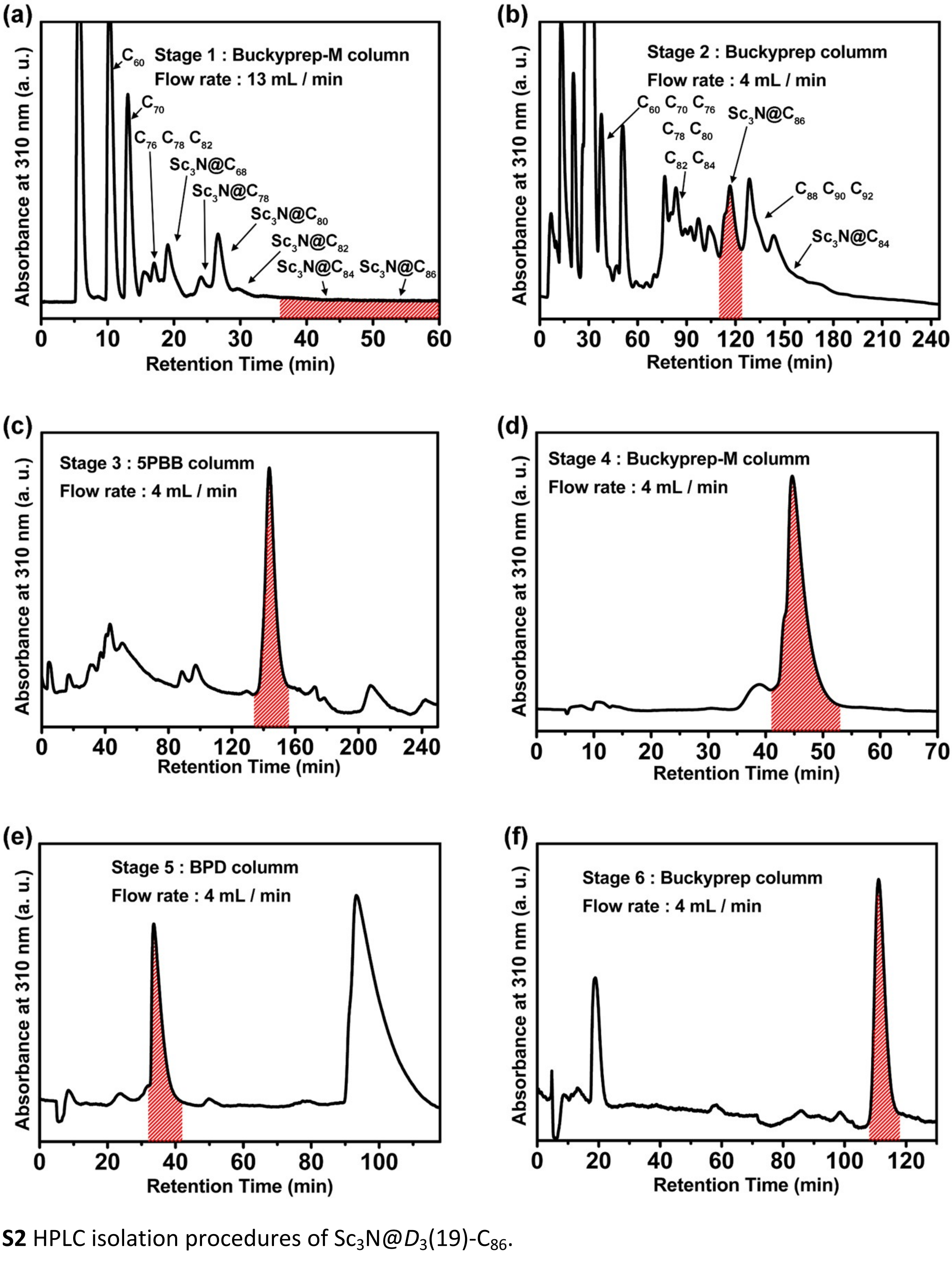

Fig. S2 HPLC isolation procedures of $Sc_3N@D_3(19)$-C_{86}.

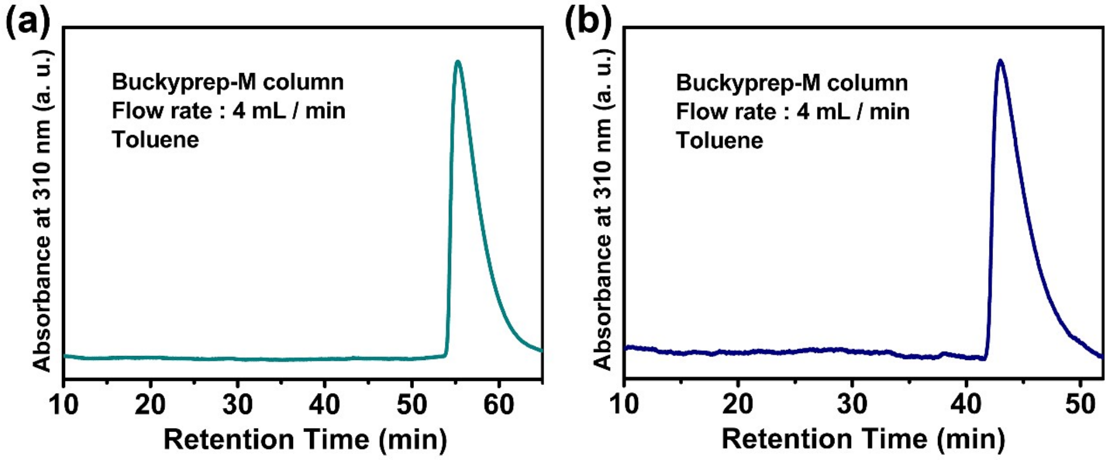

Fig. S3 HPLC chromatograms of purified (a) $Sc_3N@C_s(51365)-C_{84}$ and (b) $Sc_3N@D_3(19)-C_{86}$ on a Buckyprep-M column (10 mm × 250 mm, Cosmosil Nacalai Tesque) with toluene as the eluent. HPLC condition: λ = 310 nm, flow rate: 4 mL/min.

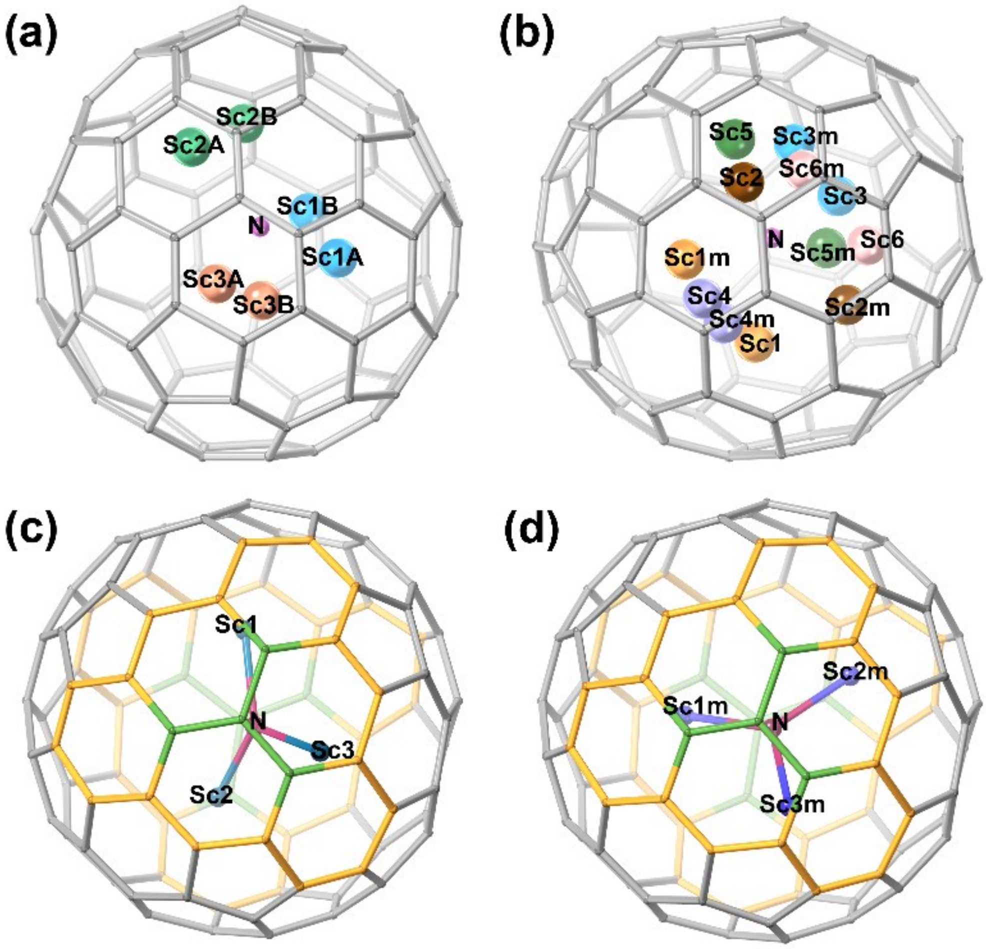

Fig. S4 Ball and stick representation of disordered scandium sites in (a) $Sc_3N@C_s(51365)\text{-}C_{84}$ and (b) $Sc_3N@D_3(19)\text{-}C_{86}$, respectively. For clarity, only the major cage orientations are shown for all EMFs. For $Sc_3N@C_s(51365)\text{-}C_{84}$, three major positions (Sc1A, Sc2A and Sc3A) and the minor sites (Sc1B, Sc2B and Sc3B) are observed. For $Sc_3N@D_3(19)\text{-}C_{86}$, six positions (Sc1, Sc2, Sc3, Sc4, Sc5 and Sc6) and the mirror-related site (Sc1m, Sc2m, Sc3m, Sc4, Sc5m and Sc6m) are observed. (C) and (D) show two sets of the Sc_3N clusters with different orientations in the major sites of the same oriented $D_3(19)\text{-}C_{86}$.

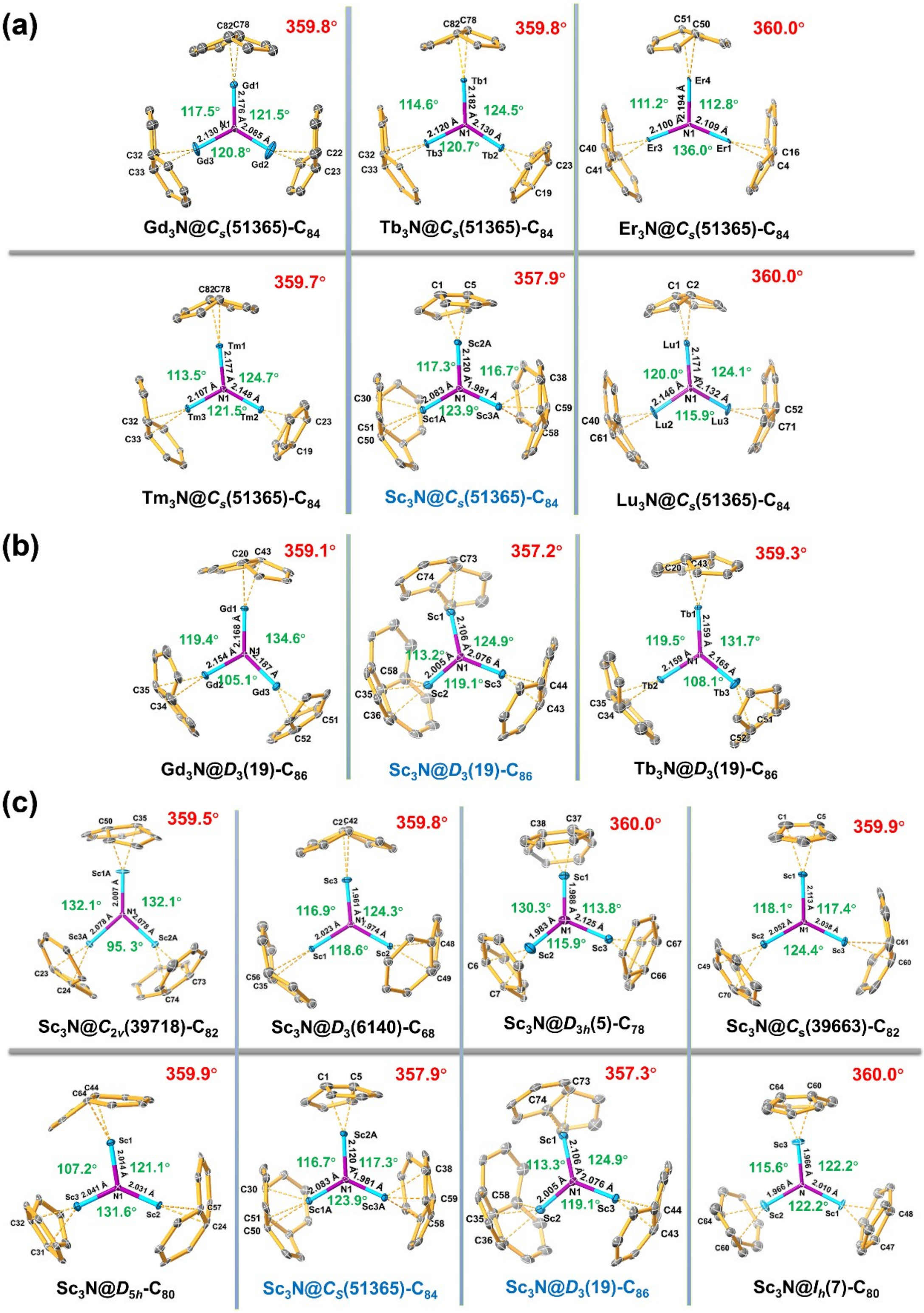

Fig. S5 A view of the relationship between the major metal nitride clusters and the closest cage portions in (a) $M_3N@C_s(51365)\text{-}C_{84}$ (M = Gd, Tb, Er, Tm, Lu and Sc)[1-4], (b) $M_3N@D_3(19)\text{-}C_{86}$ (M = Gd, Tb and Sc)[5,6] and (c) $Sc_3N@C_{2n}$ (2n = 68-86)[7-12], respectively.

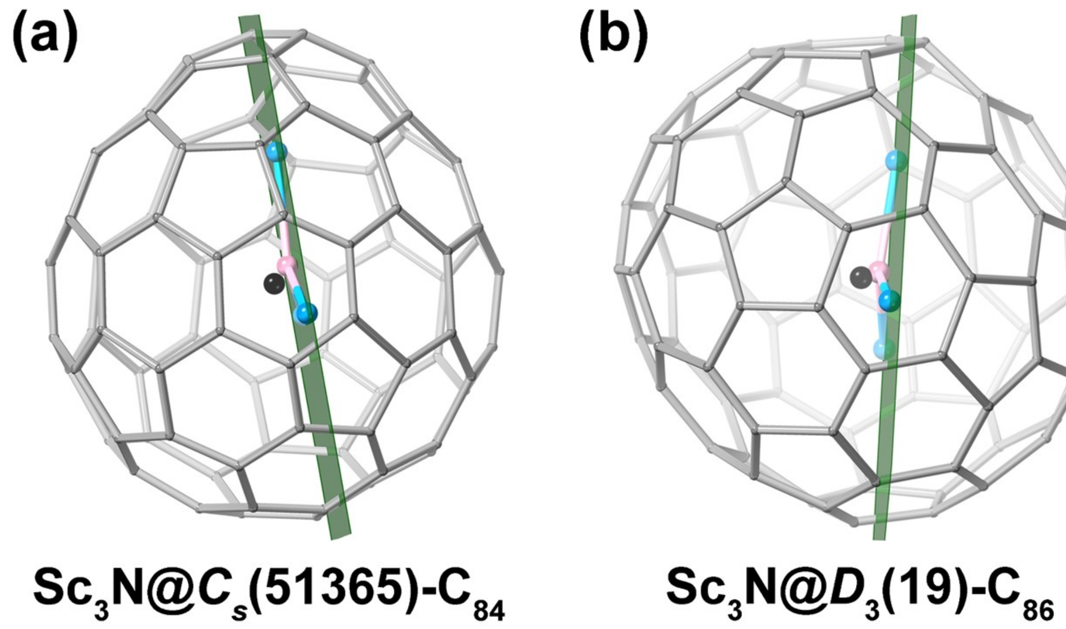

Fig. S6 Views of the Sc-triangle planes (marked in green) with respect to the center of gravity (black dots) in the carbon cage within (a) $Sc_3N@C_s(51365)\text{-}C_{84}$ and (b) $Sc_3N@D_3(19)\text{-}C_{86}$.

Crystalmaker software is used to make the center of gravity of the carbon cage (marked in black), and then make the plane of the Sc-triangle (marked in green), finally measure the distances from the center of gravity of the carbon cage to the Sc-triangle plane.

Table S1. Occupancies of disordered scandium sites in $Sc_3N@C_s(51365)-C_{84}$.

Labelling	**Sc1A**	**Sc2A**	**Sc3A**	**Sc1B**	**Sc2B**	**Sc3B**
Occupancy	0.746(4)	0.746(4)	0.746(4)	0.254(4)	0.254(4)	0.254(4)

Table S2. Occupancies of disordered scandium sites in $Sc_3N@D_3(19)-C_{86}$.

Labelling	**Sc1A**	**Sc2A**	**Sc3A**	**Sc4A**	**Sc5A**	**Sc6A**
Occupancy	0.313(3)	0.313(3)	0.313(3)	0.187(3)	0.187(3)	0.187(3)
Labelling	**Sc1B**	**Sc2B**	**Sc3B**	**Sc4B**	**Sc5B**	**Sc6B**
Occupancy	0.313(3)	0.313(3)	0.313(3)	0.187(3)	0.187(3)	0.187(3)

Table S3. Selected Interatomic Distances and Angles in $M_3N@C_s(51365)-C_{84}$ (M = Gd, Tb, Er, Tm, Lu and Sc).

	$Sc_3N@C_{84}$-C_s(51365)	$Er_3N@C_{84}$-C_s(51365)[1]	$Lu_3N@C_{84}$-C_s(51365)[2]
distance (Å)			
M1-N	2.083(6)	2.109(6)	2.171(6)
M2-N	2.120(6)	2.194(7)	2.146(6)
M3-N	1.982(6)	2.100(6)	2.132(8)
Metal-C[a]			
M1-C	2.225(8)-2.602(8)	2.286(3)-2.670(3)	2.431(2)-2.492(3)
M2-C	2.276(10)-2.413(9)	2.450(2)-2.511(2)	2.346(3)-2.651(3)
M3-C	2.266(7)-2.661(9)	2.264(2)-2.746(2)	2.331(6)-2.674(6)
Angles (deg)			
∑(M-N-M)	357.9	360.0	360.0
	$Gd_3N@C_{84}$-C_s(51365)[3]	$Tb_3N@C_{84}$-C_s(51365)[4]	$Tm_3N@C_{84}$-C_s(51365)[3]
distance (Å)			
M1-N	2.177(8)	2.182(4)	2.178(5)
M2-N	2.085(9)	2.130(4)	2.148(6)
M3-N	2.129(8)	2.120(4)	2.107(5)
Metal-C[a]			
M1-C	2.470(15)-2.547(14)	2.483(6)-2.527(6)	2.451(9)-2.518(9)
M2-C	2.399(14)-2.663(15)	2.406(6)-2.647(6)	2.395(8)-2.653(8)
M3-C	2.364(13)-2.672(13)	2.333(6)-2.660(13)	2.301(8)-2.724(15)
Angles (deg)			
∑(M-N-M)	359.8	359.8	359.7

[a] Range of distances between the metal atom and the nearest six carbon atoms.

Table S4. Selected Interatomic Distances and Angles in $M_3N@D_3(19)$-C_{86} (M = Gd, Tb and Sc).

	$Sc_3N@D_3(19)$-C_{86}	$Tb_3N@D_3(19)$-C_{86}[5]	$Gd_3N@D_3(19)$-C_{86}[6]
distance (Å)			
M1-N	2.106(7)	2.158(6)	2.168(3)
M2-N	2.005(5)	2.159(3)	2.154(2)
M3-N	2.076(6)	2.165(7)	2.187(3)
Metal-C[a]			
M1-C	2.188(15)-2.632(17)	2.454(13)-2.667(12)	2.452(6)-2.686(6)
M2-C	2.146(13)-2.503(18)	2.399(19)-2.662(15)	2.375(15)-2.629(11)
M3-C	2.088(15)-2.612(12)	2.413(14)-2.709(19)	2.360(17)-2.657(12)
Angles (deg)			
∑(M-N-M)	357.2	359.3	359.1

[a] Range of distances between the metal atom and the nearest six carbon atoms.

Table S5. Crystallographic information for $Sc_3N@C_{2n}$ (2n = 84, 86).

	$Sc_3N@C_s(51365)-C_{84}\cdot Ni^{II}(OEP)$	$Sc_3N@D_3(19)-C_{86}\cdot Ni^{II}(OEP)\cdot(C_6H_6)$
Formula weight	1749.19	1851.32
Crystal size, mm^3	0.12×0.1×0.07	0.1×0.08×0.06
Crystal system	Triclinic	Monoclinic
Space group	*P*1	*C*2/*m*
a, Å	14.6460(18)	26.259(3)
b, Å	14.9090(19)	17.9994(19)
c, Å	19.743(3)	17.8301(16)
α, deg	85.084(7)	90
β, deg	88.542(7)	108.472(4)
γ, deg	62.548(7)	90
Volume, Å3	3811.0(9)	7993.0(14)
Z	2	4
ρ, g cm^{-3}	1.524	1.538
F(000)	1780	3776
θ, deg	1.954 to 52.000	2.273 to 53.906
T, K	120(2)	120(2)
Radiation (λ, mm^{-1})	1.34139	1.34138
R_1 / wR_2 (all data)	0.1245 / 0.3112	0.1430 / 0.2667
R_1 / wR_2 ($I > 2.0\sigma(I)$)	0.1038 / 0.2927	0.0904 / 0.2305
obs reflects	9662	4504
total reflects	12883	7570
R_{int}	0.0888	0.0984
Goodness-of-fit indicator	1.057	1.057
Parameters	1199	1244
density, e $Å^{-3}$	-0.695 / 1.735	-0.445 / 0.758

Reference

1 S. Hu, P. Zhao, W. Shen, P. Yu, W. Huang, M. Ehara, Y. Xie, T. Akasaka and X. Lu, Crystallographic characterization of $Er_3N@C_{2n}$ (2n = 80, 82, 84, 88): the importance of a planar Er_3N cluster, *Nanoscale*, 2019, **11**, 13415-13422.

2 W.-Q. Shen, L.-P. Bao, S.-F. Hu, X.-J. Gao, Y.-P. Xie, X.-F. Gao, W.-H. Huang and X. Lu, Isolation and Crystallographic Characterization of $Lu_3N@C_{2n}$ (2n = 80–88): Cage Selection by Cluster Size, *Chem. - Eur. J.*, 2018, **24**, 16692-16698.

3 T. Zuo, K. Walker, M. M. Olmstead, F. Melin, B. C. Holloway, L. Echegoyen, H. C. Dorn, M. N. Chaur, C. J. Chancellor, C. M. Beavers, A. L. Balch and A. J. Athans, New egg-shaped fullerenes: non-isolated pentagon structures of $Tm_3N@C_s(51365)-C_{84}$ and $Gd_3N@C_s(51365)-C_{84}$, *Chem. Commun.*, 2008, 1067-1069, DOI: 10.1039/B716037B.

4 C. M. Beavers, T. Zuo, J. C. Duchamp, K. Harich, H. C. Dorn, M. M. Olmstead and A. L. Balch, $Tb_3N@C_{84}$: An Improbable, Egg-Shaped Endohedral Fullerene that Violates the Isolated Pentagon Rule, *J. Am. Chem. Soc.*, 2006, **128**, 11352-11353.

5 T. Zuo, C. M. Beavers, J. C. Duchamp, A. Campbell, H. C. Dorn, M. M. Olmstead and A. L. Balch, Isolation and Structural Characterization of a Family of Endohedral Fullerenes Including the Large, Chiral Cage Fullerenes $Tb_3N@C_{88}$ and $Tb_3N@C_{86}$ as well as the I_h and D_{5h} Isomers of $Tb_3N@C_{80}$, *J. Am. Chem. Soc.*, 2007, **129**, 2035-2043.

6 M. N. Chaur, X. Aparicio-Anglès, B. Q. Mercado, B. Elliott, A. Rodríguez-Fortea, A. Clotet, M. M. Olmstead, A. L. Balch, J. M. Poblet and L. Echegoyen, Structural and Electrochemical Property Correlations of Metallic Nitride Endohedral Metallofullerenes, *J. Phys. Chem. C*, 2010, **114**, 13003-13009.

7 M. M. Olmstead, A. de Bettencourt-Dias, J. C. Duchamp, S. Stevenson, D. Marciu, H. C. Dorn and A. L. Balch, Isolation and Structural Characterization of the Endohedral Fullerene $Sc_3N@C_{78}$, *Angew. Chem. Int. Ed.*, 2001, **40**, 1223-1225.

8 M. M. Olmstead, H. M. Lee, J. C. Duchamp, S. Stevenson, D. Marciu, H. C. Dorn and A. L. Balch, $Sc_3N@C_{68}$: Folded Pentalene Coordination in an Endohedral Fullerene that Does Not Obey the Isolated Pentagon Rule, *Angew. Chem. Int. Ed.*, 2003, **42**, 900-903.

9 S. Stevenson, G. Rice, T. Glass, K. Harich, F. Cromer, M. R. Jordan, J. Craft, E. Hadju, R. Bible, M. M. Olmstead, K. Maitra, A. J. Fisher, A. L. Balch and H. C. Dorn, Small-bandgap endohedral metallofullerenes in high yield and purity, *Nature*, 1999, **401**, 55-57.

10 T. Cai, L. Xu, M. R. Anderson, Z. Ge, T. Zuo, X. Wang, M. M. Olmstead, A. L. Balch, H. W. Gibson and H. C. Dorn, Structure and Enhanced Reactivity Rates of the D_{5h} $Sc_3N@C_{80}$ and $Lu_3N@C_{80}$ Metallofullerene Isomers: The Importance of the Pyracylene Motif, *J. Am. Chem. Soc.*, 2006,

128, 8581-8589.

11 T. Wei, S. Wang, F. Liu, Y. Tan, X. Zhu, S. Xie and S. Yang, Capturing the Long-Sought Small-Bandgap Endohedral Fullerene $Sc_3N@C_{82}$ with Low Kinetic Stability, *J. Am. Chem. Soc.*, 2015, **137**, 3119-3123.

12 M. Guo, X. Li, Y.-R. Yao, J. Zhuang, Q. Meng, Y. Yan, X. Liu and N. Chen, A non-isolated pentagon rule C_{82} cage stabilized by a stretched Sc_3N cluster, *Chem. Commun.*, 2021, **57**, 4150-4153.